COMPARISON OF CLOUD CLASSIFICATION METHODS

Robert Gilke, Lucas Reischmann, Steffen Ziegler, Elaheh Bastani, Sebastian Donner, Simona Ripperger-Lukošiūnaitė, Stefan Kinne, Vinod Kumar, and Thomas Wagner

Max Planck Institute for Chemistry, Satellite Remote Sensing, Germany (r.gilke@mpic.de)

Sharing is encouraged

The presentation participates in OSPP — Outstanding Student & PhD candidate Presentation contest

MAX PLANCK INSTITUTE FOR CHEMISTRY

MOTIVATION

- ➤ Cloud interference affects the light path, which is crucial for Multi-AXis Differential Optical Absorption Spectroscopy (MAX-DOAS) analyses.
- ➤ Cloud detection and classification is helpful to interpret MAX-DOAS results.
- ➤ Understanding of cloud conditions allows further insight into cloud effects on passive light DOAS observations.
- ⇒ Intercomparison of different cloud classification methods can give insight into advantages and applicability of each method.

METHOD 1: CLOUD CAMERA

Figure 1: Cloud Camera with the IR viewing angle of 30° drawn in.

The Cloud Camera is a set of two cameras, taking pictures in both the Infrared (IR) and visible (VIS) spectral ranges. In order to retrieve altitude information from the IR image (a), the greyscale value of each pixel was first converted into a temperature using laboratory measurements (b) to produce the corresponding temperature image (c). The temperature was then converted into a corresponding altitude using the following linear relationship (d):

$$h = \frac{1}{\Gamma}(T - T_0)$$

with the atmospheric lapse rate $\Gamma = -6.5\,\frac{\text{K}}{\text{km}}$ and the ground temperature T_0. This produces the altitude image (e), which can then be displayed as a histogram, showing the amount of pixels in each layer (f):

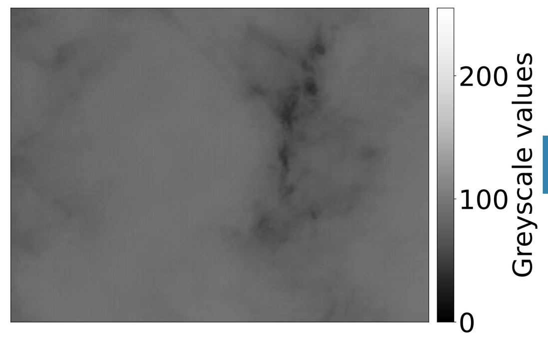

(a) Raw greyscale image.

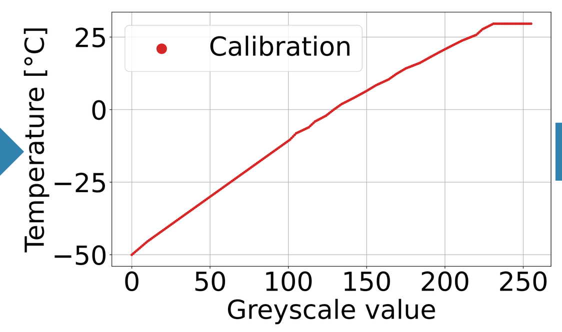

(b) Greyscale to temperature calibration.

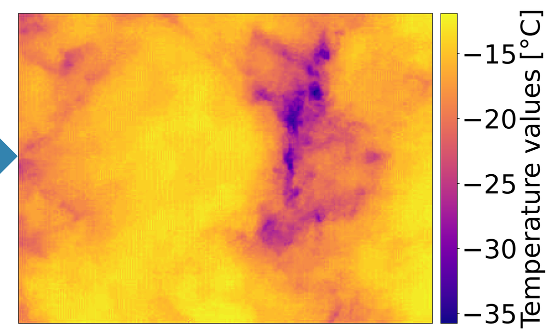

(c) Corresponding temperature values.

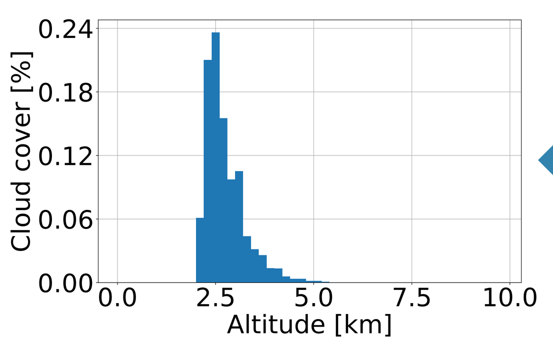

(f) Histogram showing the relative amount of each altitude.

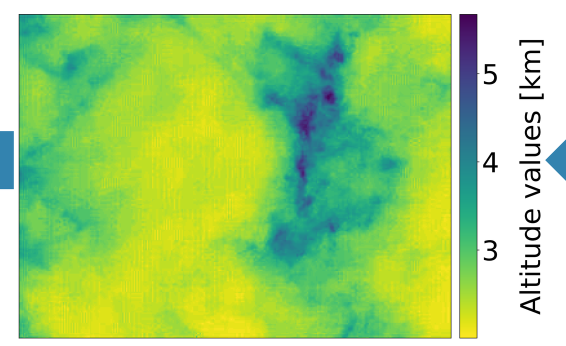

(e) Resulting altitude of clouds and background.

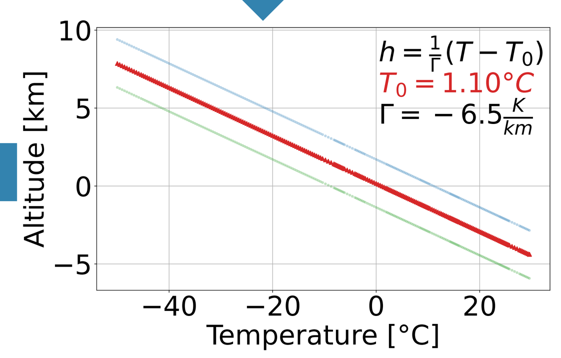

(d) Linear relationship between temperature and altitude.

Figure 2: Workflow example from raw IR image to cloud cover histogram for the 14th of February, 2025. For the linear relationship between the temperature and the altitude a ground temperature of T_0 = 1.1 °C was assumed, based on the average ground temperature for that day. This line was plottet in red while blue and green describe $T_0 \pm 10$ °C respectively.

METHOD 2: CEILOMETER

Figure 3: Rooftop Ceilometer, located next to the Cloud Camera and MAX-DOAS instrument.

In addition to the camera a Ceilometer [1] was used to classify the altitude of passing clouds. It consists of a laser emitting at 905 nm, pointed vertically into the sky. Using light detection and ranging (LIDAR) methods, the backscattered light is received and analysed to calculate the cloud base layer and the aerosol layer height used for the intercomparison.

METHOD 3: MAX-DOAS

Figure 4: Photograph of the MAX-DOAS instrument scanning at 30° elevation angle.

The third instrument employed was a MAX-DOAS instrument. It performed elevation scans from -2° to 182°, and was located next to the other two instruments.

By performing the cloud classification algorithm based on Wagner et al., 2014, 2016, 2024 [2, 3, 4], the different sky conditions can be calculated from the variations in Color Index (CI) over time.

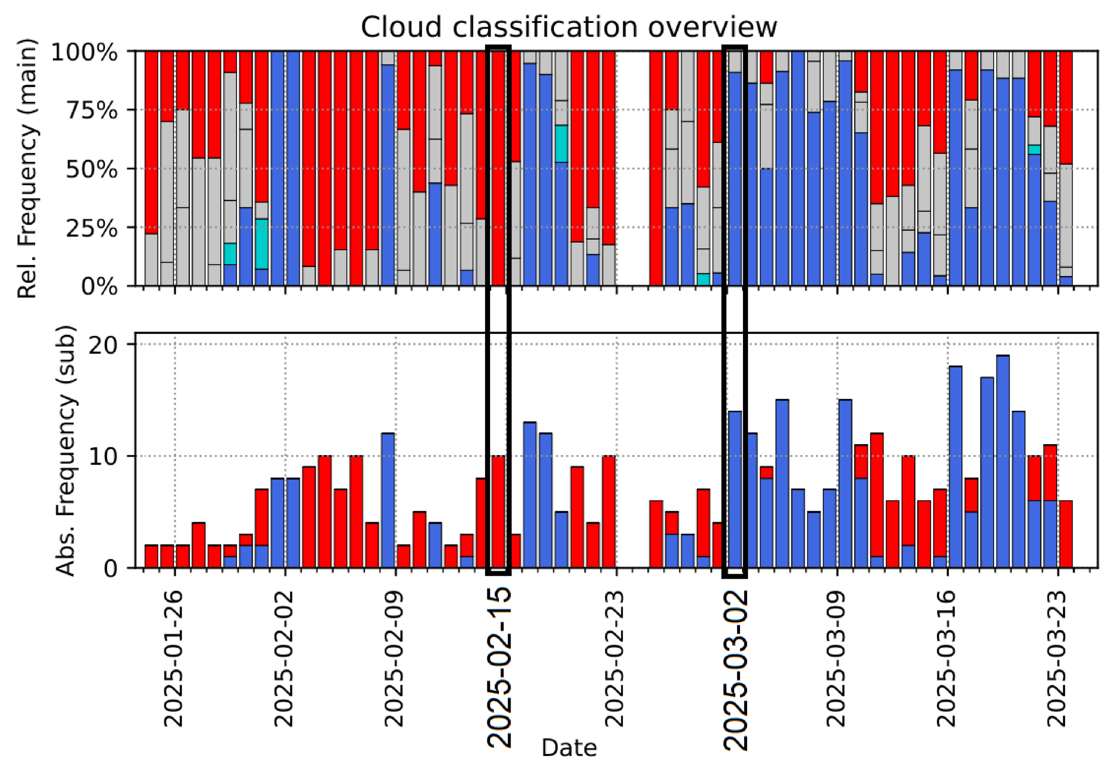

Figure 5: Relative frequency of the sky conditions during the measurement period. Red denotes continuous cloud cover, grey marks broken clouds and cloud holes, and blue indicates a clear sky. The two markings correspond to a day with continuous cloud cover (left) and a day with mostly clear sky (right).

COMPARISON: CLOUDY DAY

On a cloudy day, the cloud classification algorithm detects continuous clouds. Both the Ceilometer and the Cloud Camera provide a roughly constant altitude for the cloud bottom. The average ground temperature for this day was 0.5 °C.

The altitudes from the Ceilometer and Cloud Camera differ by about 0.8 km.

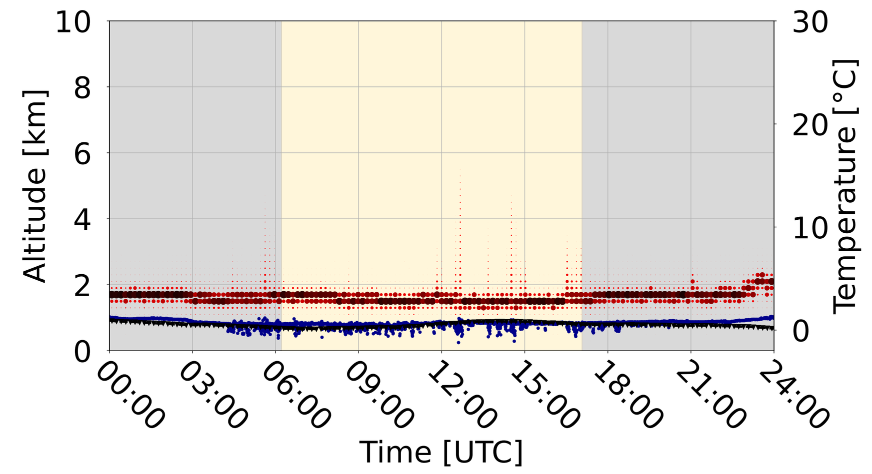

Figure 6: Timeseries of the cloud cover altitude histograms (red) and Ceilometer cloud bottom altitude (blue) for the 15th of February, 2025. Additionally, the yellow background marks daytime as defined by SZA < 90, while the **black** line describes the ground temperature timeseries. [5]

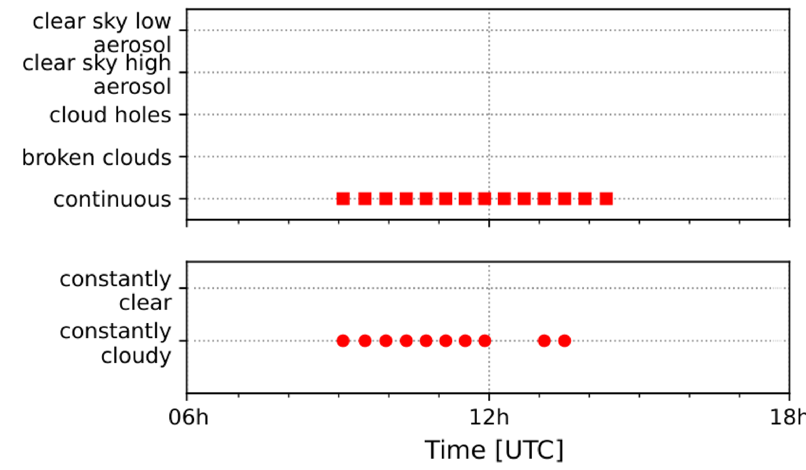

Figure 7: Results from the cloud classification algorithm for the 15th of February, 2025.

We found a strong temperature inversion in a nearby balloon sounding on this day!

POSSIBLE SOURCES OF UNCERTAINTY

- ➤ Surface temperature T_0 (d).
- ➤ Temperature profile estimated by atmospheric lapse rate Γ (d).
- ➤ Temperature calibration (b).
- ➤ Greyscale brightness (a).
- ➤ IR camera limitations (a).

COMPARISON: CLEAR DAY

On a clear day good agreement is found between the MAX-DOAS and Ceilometer results. A continuous cloud altitude of about 7.5 km is derived from the Cloud Camera.

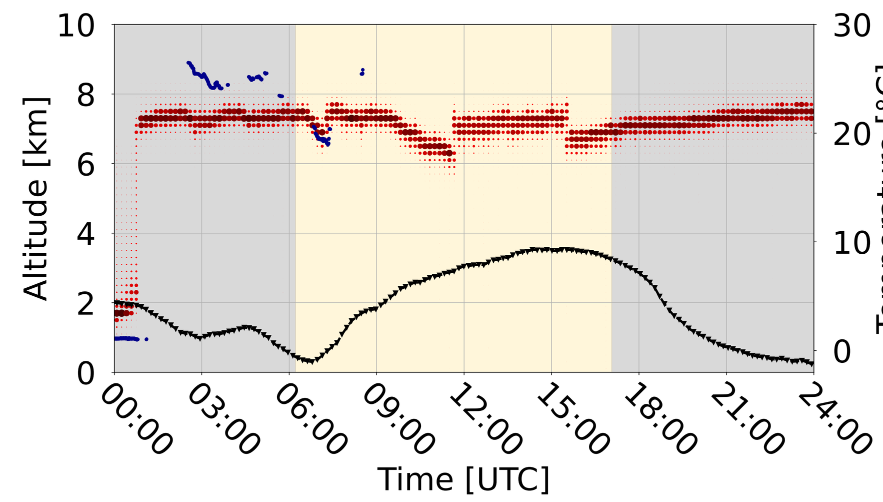

Figure 8: Altitude timeseries analogous to fig. 6 for the 2nd of March, 2025 (T_0 = 4.2 °C).

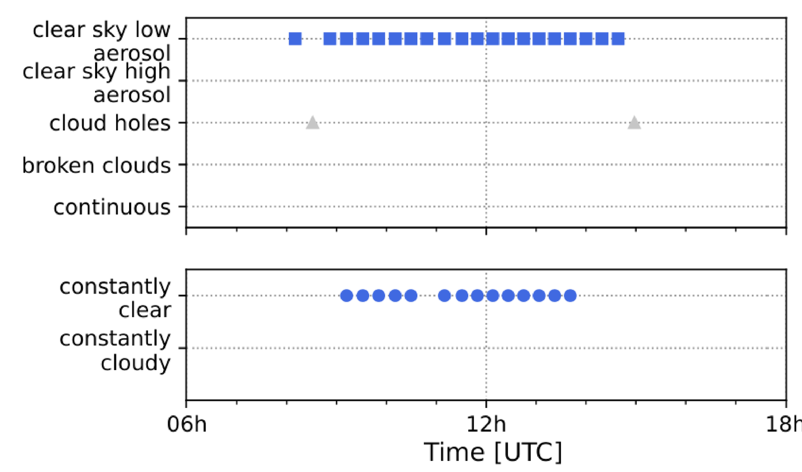

Figure 9: Results from the cloud classification algorithm for the 2nd of March, 2025.

- ➤ Partial agreement between both instruments.
- ➤ Sudden altitude increase from 12:00 UTC to 15:00 UTC.

CONCLUSION & OUTLOOK

- ➤ Cloud detection successful with all three methods.
- ➤ For the IR camera clear sky is misinterpreted as high altitude clouds.
- ⇒ Investigate the agreement between the methods for more days and in a more quantitative way.
- ⇒ Improve Cloud Camera analysis to include weather data for better agreement with cloud altitude from Ceilometer and define criteria for clear sky.
- ⇒ Investigate how far cloud altitude information can be derived from MAX-DOAS.
- ⇒ Quantify the effect of cloud cover on MAX-DOAS retrievals.

Link to Abstract

CITATIONS

[1] OTT HydroMet Fellbach GmbH. (2016). Lufft ceilometer chm 8k. https://www.lufft.com/products/cloud-height-snow-depth-sensors-288/lufft-ceilometer-chm8k-2405

[2] Wagner, T., Apituley, A., Beirle, S., Dörner, S., Friess, U., Remmers, J., & Shaiganfar, R. (2014).Cloud detection and classification based on max-doas observations. *Atmospheric Measurement Techniques*, *7*(5), 1289–1320. https://doi.org/10.5194/amt-7-1289-2014

[3] Wagner, T., Beirle, S., Remmers, J., Shaiganfar, R., & Wang, Y. (2016).Absolute calibration of the colour index and O_4 absorption derived from multi axis (max-)doas measurements and their application to a standardised cloud classification algorithm. *Atmospheric Measurement Techniques*, 9(9), 4803–4823. https://doi.org/10.5194/amt-9-4803-2016

[4] Wagner, T., Reischmann, L., Beirle, S., Ziegler, S., Piters, A., Hendrick, F., Friedrich, M., Van Roozendael, M., Richter, A., Bösch, T., Friess, U., Navarro, M., Yela, M., Bais, A., & Karagkiozidis, D. (2024).Algorithm theoretical basis document (atbd) for the cloud classification algorithm, deliverable d2.2 of the esa project fiducial reference measurements for ground-based doas air-quality observations. https://frm4doas.aeronomie.be

[5] Reutter, P. (2025). Weather data university of mainz. figshare. dataset.. https://doi.org/10.6084/m9.figshare.28760600.v3